A Thermometer-Like Mismatch Shaping Technique With Minimum Element Transition Activity for Multibit $\Delta\Sigma$ DACs

Arindam Sanyal, *Student Member, IEEE*, Peijun Wang, and Nan Sun, *Member, IEEE*

***Abstract*—This brief presents a novel mismatch shaping technique for multibit delta-sigma digital-to-analog converters (DACs). It uses the intrinsic quantization noise to randomize the element selection. Different from most existing mismatch shaping techniques that increase the element transition activity, the proposed technique keeps the same transition rate as that for the basic thermometer coding scheme. As a result, it produces much lower intersymbol interference (ISI)-induced distortions. Moreover, it does not produce tones and can high-pass shape the mismatch errors, unlike thermometer coding that produces large distortions due to static mismatch. An efficient hardware implementation based on the vector-quantizer mismatch shaping framework is also presented. Simulations show that the proposed technique can significantly improve DAC linearity in the presence of both ISI and mismatch errors.**

***Index Terms*—Analog-to-digital converter, delta-sigma ($\Delta\Sigma$) modulator, device mismatch, digital-to-analog converter (DAC), dynamic error, intersymbol interference (ISI), mismatch shaping, thermometer coding.**

I. Introduction

MULTIBIT delta-sigma ($\Delta\Sigma$) digital-to-analog converters (DACs) suffer from device mismatches that arise from layout parasitics and process nonidealities, such as gradient errors and random etching effects. The mismatch error, not shaped by the $\Delta\Sigma$ loop, causes severe linearity degradations. A way to address this issue is to use analog or digital calibration [1]–[3]. Another way is to use dynamic element matching (DEM) techniques [4]–[10]. A widely used DEM technique is to randomly scramble the element selection, which effectively turns the mismatch-induced distortion into white noise [4]. Another popular technique is data-weighted averaging (DWA) [5], [6], which does a first-order shaping of the mismatch error. Recently, more advanced techniques have been developed that can shape the mismatch errors to higher orders [7]–[10]. DEM-based approaches do not need any prior knowledge of the device mismatch unlike calibration techniques [1]–[3]. This greatly reduces the design complexity, because the accurate measurement of DAC element mismatch is nontrivial. Aside from the mismatch, another major source for distortion in a continuous-time (CT) multibit $\Delta\Sigma$ DAC is intersymbol interference (ISI), which represents the dynamic error during the switching of the DAC elements. It can be caused by asymmetric on-and-off switching, clock skew, and parasitic memory effects. Unlike the element mismatch error that shows up only in multibit DACs, ISI error exists even in a binary DAC. An analog approach to reduce the ISI error is to use the return-to-zero (RZ) scheme [11]. However, RZ signaling is highly sensitive to clock jitter and has large output discontinuities leading to increased high-frequency content in the output.

Since the DEM techniques can randomize the DAC element selection, it might seem that they could somehow mitigate the ISI problem. Unfortunately, most existing DEM techniques (e.g., [4]–[10]) actually aggravate the ISI error. This is because most DEM techniques increase the DAC element transition rate in order to quickly randomize the selection pattern, thus increasing the ISI error. The popular DWA technique has the highest switching activity and produces the largest ISI error. Recently, two novel digital techniques have been developed that can mitigate ISI errors [12], [13]. The key idea of [12] is to maintain the total number of up ($0 \rightarrow 1$) and down ($1 \rightarrow 0$) transitions of all DAC elements at a constant level independent from the input, thus turning the majority of ISI error into an offset. The technique in [13] ensures the long-term average of the DAC transition rate is kept constant, thus high-pass shaping the ISI error. Nevertheless, [13] has two drawbacks: 1) its implementation is relatively complicated; and 2) its second-order distortion increases rapidly with the input amplitude. Thus, to ensure a good distortion performance, the maximum input signal amplitude is limited to -6 dBFS, which is undesirable.

Despite its simplicity, thermometer coding has the lowest transition rate, and thus has the smallest ISI error. Element transition in thermometer coding is mainly dictated by random quantization noise, thus resulting in low ISI-induced distortion. The main drawback for thermometer coding is static mismatch issue. Recently, researchers have developed a modified thermometer coding scheme that has the same transition activity as thermometer coding but can whiten the mismatch error [14]. However, it cannot shape the mismatch error, and hence, the in-band low-frequency mismatch error is still large and limits the DAC performance. This brief presents a novel mismatch shaping technique that not only has the same lowest possible transition activity as the basic thermometer coding, but can also high-pass shape the mismatch error, thereby greatly reducing its in-band portion. It uses the intrinsic quantization noise in the $\Delta\Sigma$ modulator to randomize the DAC element selection. It also keeps track of the usage frequencies of all the elements in

Manuscript received March 12, 2014; accepted May 25, 2014. Date of publication May 29, 2014; date of current version July 16, 2014. This brief was recommended by Associate Editor E. Bonizzoni.

The authors are with the Department of Electrical and Computer Engineering, University of Texas at Austin, TX 78712 USA (e-mail: arindam3110@utexas.edu; peijun.wang@utexas.edu; nansun@mail.utexas.edu).

Color versions of one or more of the figures in this brief are available online at http://ieeexplore.ieee.org.

Digital Object Identifier 10.1109/TCSII.2014.2327342

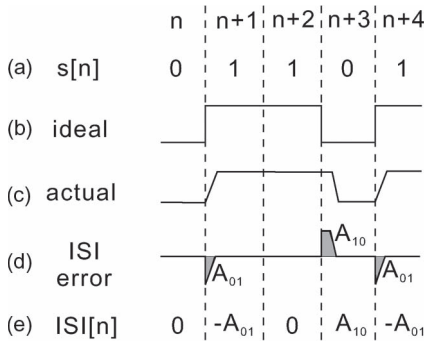

Fig. 1. (a) One-bit digital sequence. (b) Ideal DAC output. (c) DAC output with ISI error. (d) ISI error. (e) ISI sequence.

the DAC and ensures that their long-term averages are the same by using feedback. The proposed technique can be efficiently implemented using the vector-quantizer (VQ)-based mismatch shaping framework [8]. Its key innovation is that it inserts an additional loop that directly feeds the current selection pattern to the vector quantizer input. This way, it ensures that adjacent selection patterns are always maximally overlapped. To the best knowledge of the authors, it is the first technique that can high-pass shape the mismatch errors without increasing the DAC element transition rate. This brief is organized as follows. Section II reviews the ISI error model. Section III presents the proposed ISI shaping technique and discusses the simulation results. Finally, the conclusion is brought up in Section IV.

II. ISI Error Analysis and Comparison

Let us first examine the ISI error for a single 1-bit DAC. Fig. 1(a) shows an example 1-bit digital input $s[n]$. The ideal and actual DAC outputs are shown in Fig. 1(b) and (c). The ISI error pulse is plotted in Fig. 1(d).

For a low-pass $\Delta\Sigma$ DAC, what is of interest is the in-band component, i.e., the area of the ISI error pulse. Here, we use A_{01} and A_{10} to represent that for the up and down transitions. As shown in Fig. 1(e), we can derive an ISI error sequence $\{\text{ISI}[n]\}$, as shown in

$$\begin{aligned}\text{ISI}[n] &= A_{10}\left(1-s[n]\right)s[n-1] - A_{01}\left(1-s[n-1]\right)s[n] \\ &= A_{10}\left(s[n-1]-s[n]\right) + \Gamma_{01}[n](A_{10}-A_{01}) \end{aligned} \quad (1)$$

where $\Gamma_{01}[n] = (1-s[n-1])s[n]$ and represents the up transition. The first term of (1) represents a first-order difference of $s[n]$ and, thus, is linear. The second term is proportional to $\Gamma_{01}[n]$, which is nonlinear. Thus, the ISI nonlinearity can be associated with the up transition. It can be mathematically shown that the ISI nonlinearity can be associated with any one of the four possible transitions $(0 \to 0)$, $(0 \to 1)$, $(1 \to 0)$, and $(1 \to 1)$. For example, using (1), ISI$[n]$ can be rewritten as $(A_{01} - A_{10})(s[n-1]s[n]) + A_{10}(s[n-1]) - A_{01}(s[n])$ with the ISI nonlinearity being associated to the $(1 \to 1)$ transition. The key message is that ISI nonlinearity can be substantially reduced if only one of the four transition densities is reduced a lot [13]. In the analog domain, RZ signaling does this by ensuring that there is no $(1 \to 1)$ transition. Since thermometer coding has the minimum up-transition density $\Gamma_{01}[n]$, it is expected that it produces the smallest ISI nonlinearity. By contrast, DWA has the highest transition rate and thus produces the largest ISI nonlinearity. For a multibit DAC with M elements, the total ISI error sequence is given by the summation of all individual ISI sequences. Thus, the overall DAC ISI nonlinearity is proportional to the total number of up transitions, given by

$$\Gamma[n] = \sum_{i=1}^{M} \Gamma_{01i}[n] \quad (2)$$

where $\Gamma_{01i}[n]$ represents the up-transition sequence for the ith element.

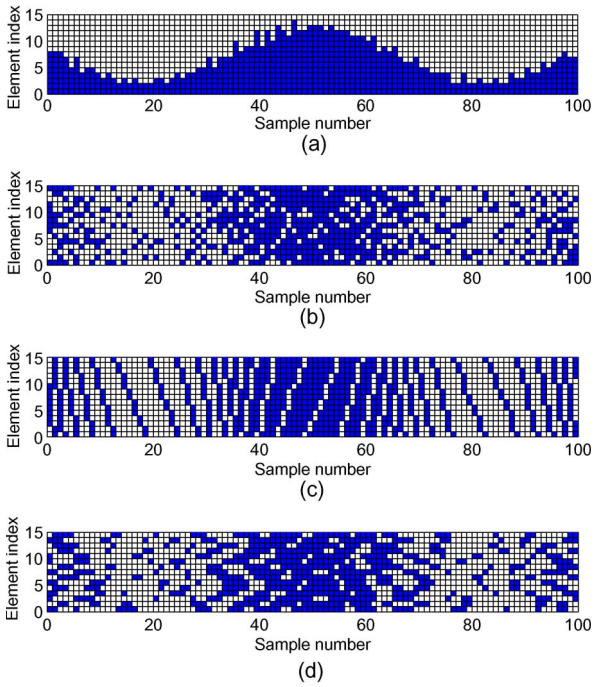

Fig. 2. Selection pattern for (a) thermometer, (b) DEM, (c) DWA, and (d) ISI shaping.

Now, let us compare the ISI errors for thermometer coding, DEM, DWA, and the ISI shaping technique of [13]. Fig. 2 shows their simulated element selection patterns for a 15-element third-order $\Delta\Sigma$ DAC with a noise transfer function (NTF) of $(z-1)(z^2-1.994z+1)/(z-0.2782)(z^2-0.3593z+0.2031)$ and a -3 dBFS input. A solid box means that its corresponding unit-element DAC is on, and an empty box means it is off. Figs. 3 and 4 show the simulated total up-transition sequence $\Gamma[n]$ in time and frequency domains, respectively. It is clear that thermometer coding, despite its simplicity, has the lowest transition rate and no appreciable distortions [see Figs. 3(a) and 4(a)]. DEM has a higher transition rate and an obvious second-order distortion [see Figs. 3(b) and 4(b)]. DWA produces the largest transition rate and the biggest second-order distortion [see Figs. 3(c) and 4(c)]. The ISI shaping technique maintains a long-term constant number of element transitions, and thus, can high-pass shape the spectrum of $\Gamma[n]$; however, it still produces a large second-order harmonic [see Figs. 3(d) and 4(d)].

In summary, the simulation results clearly show that thermometer coding produces the lowest ISI-induced harmonic distortions among these techniques. Nevertheless, it has an obvious drawback of being prone to mismatch errors. The key contribution of this brief is that we propose a novel mismatch shaping technique that has the same transition rate and ISI performance as thermometer coding but can shape the static mismatch errors as well.

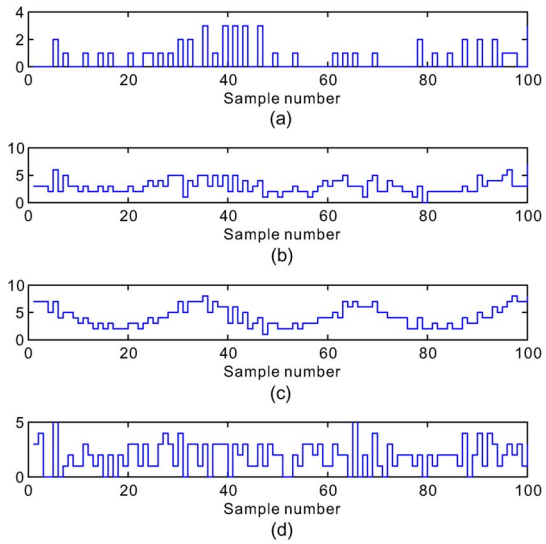

Fig. 3. Up-transition pattern $\Gamma[n]$ for (a) thermometer, (b) DEM, (c) DWA, and (d) ISI shaping.

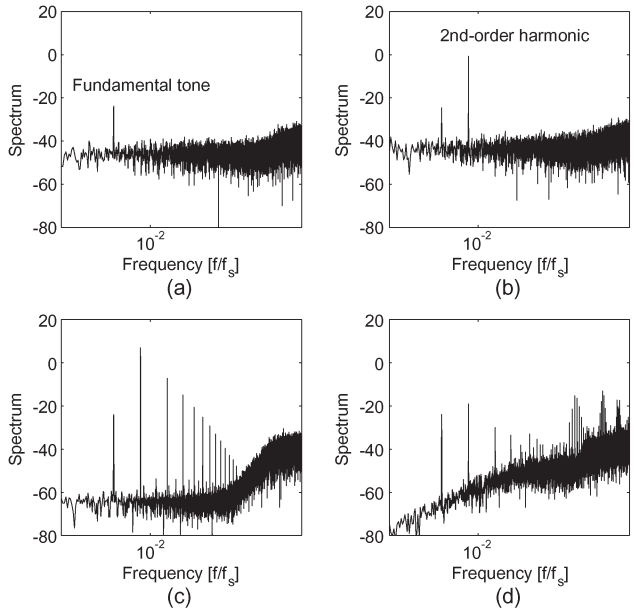

Fig. 4. Spectrum of $\Gamma[n]$ for (a) thermometer, (b) DEM, (c) DWA, and (d) ISI shaping.

III. Proposed Thermometer-Like Mismatch Shaping Technique

The function of any mismatch shaping technique is to convert a multibit quantizer output $v[n]$ into vector $\vec{sv}[n]$, of which each binary element controls a unit-element DAC. Depending on the relationship between $v[n]$ and $v[n-1]$, the operation of the proposed technique can be divided into three different cases.

1) If $v[n] = v[n-1]$, no change in the element selection pattern.
2) If $v[n] > v[n-1]$, turn on $(v[n] - v[n-1])$ unselected elements that have been least frequently used.
3) If $v[n] < v[n-1]$, turn off $(v[n-1] - v[n])$ selected elements that have been most frequently used.

This way, adjacent selection patterns are always maximally overlapped. As a result, its transition activity is as low as thermometer coding. In addition, since we always turn on the least frequently used elements and turn off the most frequently used elements, it is expected that long-term usage frequencies for all elements are the same. As a result, the in-band low-frequency portion of $\vec{sv}[n]$ is very small, leading to the high-pass shaping of the mismatch errors.

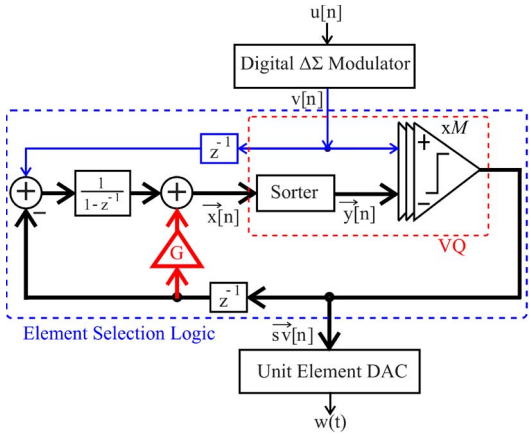

Fig. 5. Block diagram for the proposed mismatch shaping technique.

To implement such a selection scheme, we need to record previously selected elements, keep a log of how many times each DAC element has been used, and rank them accordingly. An efficient way to implement such an algorithm is shown in Fig. 5. The thick lines indicate vectors with the length of M. The architecture builds upon the standard VQ-based mismatch shaping framework, in which the integrator $1/(1-z^{-1})$ records how many times each element has been used [8]. The key difference is that a direct feedback path with a gain G is inserted. G is selected to be large enough (e.g., $G = 100$), so that the direct feedback path dominates the integration path. As a result, previously selected elements always have the highest priority to be selected again, thus ensuring the lowest transition rate possible. The usage frequency information (the integrator output) matters only when elements need to be turned on or off (i.e., $v[n] \neq v[n-1]$).

Note that the upper path in Fig. 5 is added to ensure that the average value of the vector integrator output is always fixed [10]. It reduces the hardware complexity by removing the need for an additional block to subtract out the smallest value of the integrator output, as is required in the conventional VQ-based mismatch shaping loop [8]. The sorter ranks the output of the filters, and the elements that have rank lower than $v[n]$ are selected in the next cycle. The sorter architecture is discussed in more detail in [16].

There is a design tradeoff in the choice of G. If $G = 0$, the proposed technique is equivalent to a first-order VQ, or DWA, which shapes the static mismatch error. However, this also increases the element transition rate, which results in large dynamic errors. If G is assigned a high value, the element transition rate, and hence, the ISI error is reduced. This is also confirmed through simulations on a 15-element DAC for different static mismatch and ISI errors, as shown in Table I. The simulation conditions are the same as used for simulations in Fig. 2. As can be seen from Table I that if static mismatch is the main source of error, then low value of G maximizes the signal-to-noise-and-distortion ratio (SNDR), whereas a higher value of G is needed for maximizing SNDR in presence of ISI error. At high values of G, the SNDR flattens out and does not provide any more improvement. This is because if

TABLE I
VARIATION OF UP-TRANSITION DENSITY AND SNDR WITH G

	G					
SNDR(dB)	0	0.1	1	10	100	1000
0.1% static, 0.1% ISI	66	73.5	77.4	72.4	71.4	71.4
0.5% static, 0.1% ISI	67.4	74.9	78.8	80.8	79.9	79.9
0.1% static, 0.5% ISI	53.3	60.7	64.7	72.1	71.7	71.7
0.3% static	103.1	99.7	95	73.8	72.9	72.9
0.3% ISI	58.5	66	69.9	77.7	77.5	77.5
up-transition density	0.28	0.19	0.13	0.05	0.05	0.05

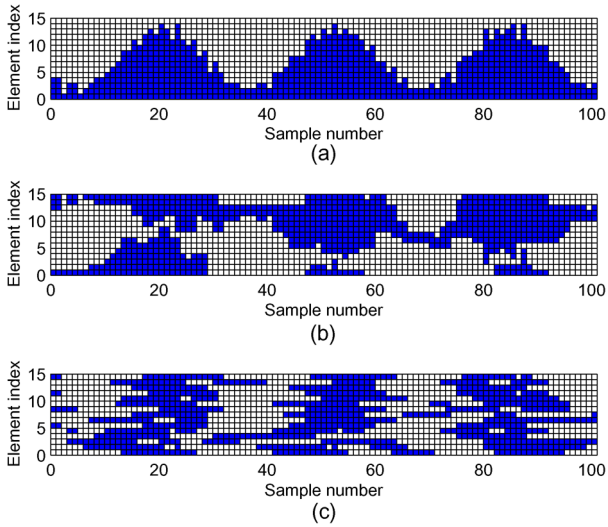

Fig. 6. Element selection pattern for (a) thermometer coding, (b) technique of [14], and (c) proposed technique.

G is very big, the direct feedback path always dominates, and thus, the element transition patterns are always identical. It can be also seen from Table I, that if static mismatch is the only source of DAC error, increasing G reduces the SNDR. This is because, with increase of G, the element transition density starts approaching that of thermometer coding. This can be also seen from Table I, which clearly shows reduction of element up-transition density as G increases. The up-transition density is eventually flattened at high values of G as the transition density becomes close to the transition density of thermometer coding.

Fig. 6 shows the simulated selection pattern $\vec{sv}[n]$ for thermometer coding, the technique of [14], and the proposed technique. Note that the spectrum of $\vec{sv}[n]$ refers to the spectrum of $sv_i[n]$ $(i \in [1, M])$, averaged over all the elements. All of these three coding schemes have the same element transition activity $\Gamma[n]$, but the selection pattern $\vec{sv}[n]$for the proposed technique is more random. It also ensures that the total number of usages for all elements is the same. Fig. 7 shows the normalized spectrum of $\vec{sv}[n]$. It can be seen that there are large harmonics for thermometer coding, because its element selection pattern is highly correlated with the input. By contrast, both spectra for the technique of [14] and the proposed technique show no harmonics due to randomization in the selection pattern. The advantage of the proposed technique is that it can high-pass shape the mismatch error and have much smaller in-band low-frequency components than that of [14]. To get an understanding of the noise-shaping characteristic of the proposed technique, let us model the VQ by a linear gain K and a quantization error ϵ. Thus

$$sv = \left(\frac{z^{-1}}{1-z^{-1}}(v - sv) + Gz^{-1}sv\right)K + \epsilon$$

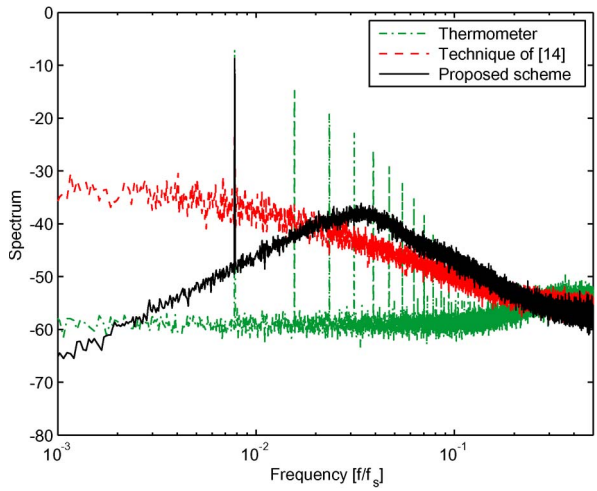

Fig. 7. Spectra of $\vec{sv}[n]$.

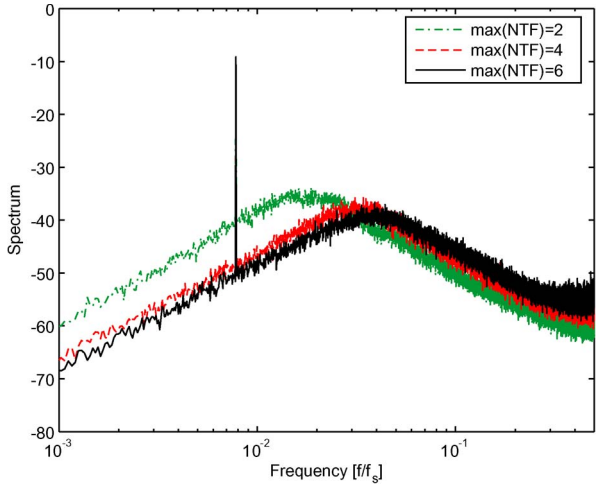

Fig. 8. Spectra of $\vec{sv}[n]$ for different maximum NTF gains.

$$\begin{aligned} \Longrightarrow sv &= \left(\frac{z^{-1}K}{1+(K-1-GK)z^{-1}+GKz^{-2}}\right)v \\ &\quad + \left(\frac{1-z^{-1}}{1+(K-1-GK)z^{-1}+GKz^{-2}}\right)\epsilon \\ &\equiv H_1(z)v + H_2(z)\epsilon. \end{aligned} \tag{3}$$

It can be seen from (3) that $H_2(z)$ has a first-order shaping at low frequencies and a low gain at high frequencies. This can be also seen from the spectrum in Fig. 7.

The randomization in the element selection of the proposed technique only happens when there is a change in $v[n]$, which heavily depends on the quantization noise. Thus, it is expected that the overall mismatch shaping effect varies with the amount of quantization noise. Fig. 8 shows the spectra of $\vec{sv}[n]$ as a function of the maximum gain of the NTF for the $\Delta\Sigma$ modulator. It is clear that as the maximum NTF gain increases, the mismatch shaping result improves. The reason is that the proposed technique essentially uses the intrinsic quantization noise to randomize $\vec{sv}[n]$. Thus, more quantization noise leads to a more randomization effect and a better mismatch shaping result. Consequently, the proposed technique works better for $\Delta\Sigma$ DACs with aggressive NTFs.

Fig. 9 shows the output spectra of a fifth-order 32-element $\Delta\Sigma$ DAC with an NTF of $((z-1)(z^2-1.99z+1)(z^2-1.998z+1)/(z-0.3541)(z^2-0.6847z+0.1693)(z^2-0.6614z+$

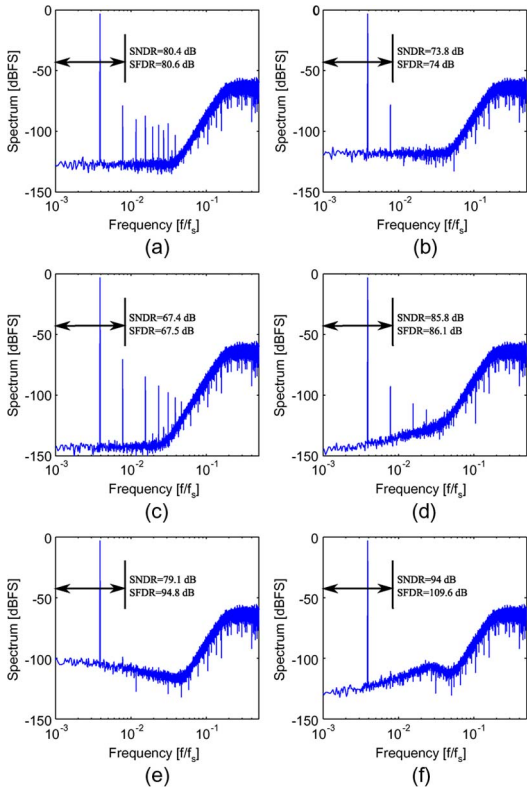

Fig. 9. DAC output spectrum for (a) thermometer coding, (b) DEM, (c) DWA, (d) ISI shaping, (e) technique of [14], and (f) proposed technique.

0.4616)) for various coding schemes. The maximum NTF gain is set to be 6. Both the static mismatch error and the dynamic ISI error are assumed to be 0.1%. The input amplitude is -3 dBFS. A full signal swing is not used to ensure the stability of the $\Delta\Sigma$ modulator. The basic thermometer coding is prone to device mismatches and thus produces many harmonics and achieves a spurious-free dynamic range (SFDR) of 80.6 dB [see Fig. 9(a)]. DEM scrambles the mismatch errors into white noise but produces a large second-order harmonic (SFDR of 74 dB) due to ISI error [see Fig. 9(b)]. DWA can achieve very low noise floor, but it produces the largest ISI-induced distortion, and its SFDR worsened to 67.5 dB [see Fig. 9(c)]. The ISI shaping technique effectively reduces the ISI-induced distortion, but it still produces obvious harmonic tones, and its SFDR is 86.1 dB [see Fig. 9(d)]. Both the technique of [14] and the proposed technique produce no appreciable harmonics because both of them can randomize the DAC element selection pattern while ensuring the same minimum transition rate as thermometer coding. Compared with [14], the advantage of the proposed technique is that it can achieve the first-order shaping of the mismatch error and substantially lower the in-band noise floor. At an oversampling ratio of 64, the SNDR for the proposed technique is 94 dB, which is 15 dB higher than that of [14], whose SNDR is 79 dB. In summary, the proposed technique achieves the best performance in the presence of both mismatch and ISI errors.

IV. Conclusion

This brief presented a novel mismatch shaping technique for CT low-pass $\Delta\Sigma$ DACs. It can be also used in multi-bit $\Delta\Sigma$ analog-to-digital converters to address the nonlinearity problem in the feedback DACs. Compared with existing mismatch shaping techniques, it can significantly reduce the distortions due to both static mismatches and dynamic ISI errors. It is particularly useful for applications that demand high linearity, such as the high-quality audio applications. As a purely digital technique, it is scaling friendly and is expected to consume negligible area and power in deep-submicron CMOS processes.

References

[1] U. Moon, J. Silva, J. Steensgaard, and G. C. Temes, "A switched-capacitor DAC with analog mismatch corrections," *Electron. Lett.*, vol. 35, no. 22, pp. 1903–1904, Oct. 1999.

[2] R. T. Baird and T. S. Fiez, "A low oversampling ratio 14-b delta-sigma ADC with self-calibrated multibit DAC," *IEEE J. Solid-State Circuits*, vol. 31, no. 3, pp. 312–320, Mar. 1996.

[3] M. De Bock, X. Xing, L. Weyten, G. Gielen, and P. Rombouts, "Calibration of DAC mismatch errors in $\Delta\Sigma$ ADCs based on a sine-wave measurement," *IEEE Trans. Circuits Syst. II, Exp. Briefs*, vol. 60, no. 9, pp. 567–571, Sep. 2013.

[4] R. J. Van De Plassche, "Dynamic element matching for high accuracy monolithic D/A converters," *IEEE J. Solid-State Circuits*, vol. SC-11, no. 6, pp. 795–800, Dec. 1976.

[5] H. S. Jackson, "Circuit and method for cancelling nonlinearity error associated with component value mismatches in a data converter," U.S. Patent 5 221 926, Jun. 22, 1993.

[6] R. T. Baird and T. S. Fiez, "Linearity enhancement of multibit $\Sigma\Delta$ A/D and D/A converters using data weighted averaging," *IEEE Trans. Circuits Syst. II, Analog Digit. Signal Process.*, vol. 42, no. 12, pp. 753–762, Dec. 1995.

[7] N. Sun, "Mismatch-shaped segmented multibit $\Delta\Sigma$ DACs," *IEEE Trans. Circuits Syst. I, Reg. Papers*, vol. 59, no. 2, pp. 295–304, Feb. 2012.

[8] R. Schreier and B. Zhang, "Noise-shaped multibit D/A convertor employing unit elements," *Electron. Lett.*, vol. 31, no. 20, pp. 1712–1713, Sep. 1995.

[9] I. Galton, "Spectral shaping of circuit errors in digital-to-analog converters," *IEEE Trans. Circuits Syst. II, Analog Digit. Signal Process.*, vol. 44, no. 10, pp. 808–817, Oct. 1997.

[10] N. Sun, "High-order mismatch shaping in multi-bit $\Delta\Sigma$ DAC," *IEEE Trans. Circuits Syst. II, Exp. Briefs*, vol. 58, no. 6, pp. 346–350, Jun. 2011.

[11] K. Nguyen, R. Adams, and K. Sweetland, "A 113 dB SNR oversampling Sigma-Delta DAC for CD/DVD application," *IEEE Trans. Consum. Electron.*, vol. 44, no. 3, pp. 1019–1023, Aug. 1998.

[12] T. Shui, R. Schreier, and F. Hudson, "Mismatch shaping for a current-mode multi-bit delta-sigma DAC," *IEEE J. Solid-State Circuits*, vol. 34, no. 3, pp. 331–338, Mar. 1999.

[13] L. Risbo, R. Hezar, B. Kelleci, H. Kiper, and M. Fares, "Digital approaches to ISI-mitigation in high-resolution oversampled multi-level D/A converters," *IEEE J. Solid-State Circuits*, vol. 46, no. 12, pp. 2892–2903, Dec. 2011.

[14] M. H. Shen, J. H. Tsai, and P. C. Huang, "Random swapping dynamic element matching technique for glitch energy minimization in current-steering DAC," *IEEE Trans. Circuits Syst. II, Exp. Briefs*, vol. 57, no. 5, pp. 369–373, May 2010.

[15] K. O. Andersson and M. Vesterbacka, "Modeling of glitches due to rise/fall asymmetry in current-steering digital-to-analog converters," *IEEE Trans. Circuits Syst. I, Reg. Papers*, vol. 52, no. 11, pp. 2265–2275, Nov. 2005.

[16] N. Sun and P. Cao, "Low-complexity high-order vector-based mismatch shaping in multi-bit $\Delta\Sigma$ ADCs," *IEEE Trans. Circuits Syst. II, Exp. Briefs*, vol. 58, no. 12, pp. 872–876, Dec. 2011.